Journal of Fluids and Structures (1999) **13,** 399–418
Article No.: jfls.1999.0207 available online at http://www.idealibrary.com on IDEAL

FLOW LIMITATION IN UNIFORM THICK-WALLED COLLAPSIBLE TUBES†

C. D. BERTRAM AND R. J. CASTLES

Graduate School of Biomedical Engineering, University of New South Wales Sydney, Australia 2052

(Received 16 August 1998 and in revised form 10 November 1998)

To investigate the flow-rate limitation behaviour of the same thick-walled silicone-rubber tubes with aqueous flow as have previously been characterized by this laboratory in terms of their pressure-drop limitation behaviour, we measured how the pressure drop along the tube varied with flow rate, when both the upstream head and the external pressure were varied in such a way as to keep the transmural pressure at the upstream end to the tube at a series of constant values. Flow limitation with 'negative effort dependence' occurred, and it was found that the flow rate depended not just on the upstream transmural pressure but also on its history, in a hysteretic manner. Furthermore, when external pressure was being reduced to the required point, either flow limitation or absence of collapse could be obtained for the same values of upstream transmural pressure. The reductions in flow rate when flow limitation came into effect were typically much greater, relative to the flow-limited flow rates themselves, than has been reported by others using thinner tubes and lower flow rates. Large-amplitude self-excited oscillation was confined to this reducing-flow-rate transition when external pressure was being increased to set the required point, and largely confined to this transition when it was being reduced. Flow limitation was mostly associated with only small-amplitude noise-like fluctuations of the downstream pressure. The transition was analysed and explained by reference to modified control-space diagrams, which show explicitly all oscillatory and divergent instabilities as closed regions. The prominence of the transition in these results forced consideration of whether flow limitation occurs when the flow rate ceases to increase or when it becomes substantially independent of the pressure drop. In adopting the latter definition, we were led to hypothesize that the initial collapse-inducing instability is not the result of choking.

1. INTRODUCTION

A FLEXIBLE TUBE CONVEYING a flow is a system in which there can be strong coupling between the fluid flow within the tube, the pressure gradients driving that flow, and the shape of the tube itself, forming the flow boundary. The coupling is weak while the tube is distended, but strong when the tube collapses to noncircular cross-sectional shapes as the result of external pressure greater than that within. Under these conditions, such a system can exhibit two unusual and physiologically important phenomena: flow-rate limitation (Shapiro 1977a) and self-excited oscillation. Flow-rate limitation by this mechanism occurs in the pulmonary airways, during forced expiration, and in the urethra, during micturition. It is also implied in the control of cardiac output by venous return (Guyton & Adkins 1954). Flow limitation in the context of pulmonary expiration was first demonstrated by Fry *et al.*

†Parts of this work were presented at the ASME Summer Bioengineering Conference, 11–15 June 1997, Sunriver, Oregon, U.S.A., and at the Third World Congress of Biomechanics, 2–8 August 1998, Sapporo, Japan.

0889–9746/99/040399 + 20 $30.00

(1954), and the now well-known flow–volume curve which shows how the maximum expiratory flow varies with lung volume was devised by Hyatt *et al.* (1958). Another situation where overmuch reduction of downstream pressure by pumping leads to vessel collapse rather than increased flow rate occurs in renal dialysis. Sustained self-excited oscillation is apparently avoided in the body's conduits, except in specialized organs such as the larynx (and the syrinx of a bird), but transient oscillation is reasonably common (Shapiro 1977b).

However, in the body, the conditions needed for flow limitation are only approximated. In the laboratory, where they can be precisely regulated, experiments on flow limitation have commonly encountered tube oscillation. Flow limitation in collapsible tubes can occur by two different mechanisms, one of which, depending only on viscous pressure drop, can operate at low Reynolds numbers where self-excited oscillation is not possible. However, at the substantial Reynolds numbers of the physiological examples above, where limitation is probably by the wavespeed mechanism, it is often assumed that the two behaviours are associated, and it has sometimes been argued that they are causally linked, i.e. that high-Reynolds-number flow limitation is a necessary and sufficient condition for oscillation. This viewpoint is reinforced by the audible occurrence of wheezing during forced expiration. Much of the experimental evidence bearing on this issue comes from extremely thin-walled tubes with tiny bending stiffness, in which elastic restoring forces come primarily from longitudinal stretch during collapse. However, much thicker flexible tubes, in which the elastic restoring force is predominantly local bending stiffness, share qualitatively the same collapse dynamics. We have previously thoroughly characterized the pressure-drop limitation behaviour of rather thicker-walled collapsible tubes than those used elsewhere. We have now investigated the flow limitation behaviour of these same tubes, seeking to understand the processes at work and the oscillation modes involved through use of control–space diagrams.

2. METHODS

Our methods have been described at length in past publications [see Bertram *et al.* (1991), and references therein]. The tubing used was of silicone rubber, of unpressurized internal diameter 13 mm and wall thickness 2·4 mm; the unsupported length was 17 internal diameters. The fluid was water (with inorganic solutes for controlling pH, corrosion and ionic conductivity). Data from transducers measuring pressures and flow rates were recorded manually, by chart recorder and digitally. We have previously shown, in accord with experiments elsewhere on thinner tubes, that pressure-drop limitation is exhibited when the time-averaged pressure/flow-rate tube operating points are examined as curves of $\bar{Q}$ versus $\bar{p}_{12} = \bar{p}_1 - \bar{p}_2$ at constant values of $\bar{p}_{e2} = p_e - \bar{p}_2$, where Q is the volume flow rate, p the pressure, and suffixes 1, 2, and e denote just upstream of, just downstream of, and external to the tube respectively; an overbar denotes the time average of a time-varying quantity. Desired values of $\bar{p}_{e2}$ are achieved by adjusting p_e after setting the upstream head (p_u). Unlike others, however, we also use values of $\bar{p}_{e2}$ to construct a control–space diagram, which shows explicitly all the modes of oscillation possible for a given tube.

The terminology "control–space diagram" is taken from dynamical systems analysis practice. Strictly, the control–space diagram plots the results, in terms of regions of qualitatively distinct dynamical behaviour, of investigating the space defined by the control parameters. These are the quantities directly under the experimenter's control. In the case of a collapsible tube as investigated here, these parameters are p_u and p_e. Yamane & Orita (1994b) used instead $\bar{Q}$ (which depends on p_u) and p_e to construct a kind of control space. However, we previously demonstrated (Bertram *et al.* 1991) a particular advantage in

plotting instead a modified control–space diagram, using the dependent variable $\bar{p}_{e2}$ instead of the independent p_e. The advantage is that the diagram then includes not only regions corresponding to all oscillatory modes, but also so-called unattainable zones corresponding to the absence of a stable (steady or oscillatory) operating point for the requisite $(p_u, \bar{p}_{e2})$ combination. (For an example of such a diagram, the reader is referred forward to Figure 2 in the Results section.) Were we to plot p_e instead, these zones of divergent instability would shrink to mere boundaries between stable regions and be indistinguishable on the diagram from a simple continuous (gradual) transition between two such stable modes. A secondary advantage is to expand the operating-point range in which varying modes occur over a convenient area of graph space; on (p_u, p_e)-space this range is confined to a narrow area around the positive diagonal, because p_e has necessarily to balance p_u to provide moderate degrees of collapse. (This problem alone could of course be overcome differently, by use of a coordinate transformation scheme.) For our modified control–space, varying p_e (and thereby $\bar{p}_{e2}$) after setting p_u amounts to investigating only constant-p_u lines across the diagram. The existence of the two-dimensional regions corresponding to different modes is inferred from similarities between the results gained at those p_u-lines closest to each other. The data which are needed for the construction of the control–space diagram are those threshold values of $\bar{p}_{e2}$ (at a number of different, approximately equi-spaced values of p_u) at which the behaviour of the tube changes. Because this nonlinear system displays much hysteresis (Bertram *et al.* 1990), the thresholds are not located at the same values of $\bar{p}_{e2}$ when p_e is being increased as when it is being decreased, and in fact there are sometimes additional or missing modes altogether, depending on the direction of approach to the $\bar{p}_{e2}$ value. We therefore find it necessary to construct two separate diagrams, one for each direction of p_e movement, as did Bertram & Butcher (1992).

Demonstration of flow-rate limitation requires instead that curves of $\bar{Q}$ versus $\bar{p}_{12}$ at constant values of $\bar{p}_{e1} = p_e - \bar{p}_1$ be obtained. As when setting operating points in terms of $\bar{p}_{e2}$, p_e was adjusted to reach the required $\bar{p}_{e1}$ after setting p_u. For each constant-$\bar{p}_{e1}$ curve, seven or eight standard values of p_u in the range 13–200 kPa were initially investigated, then further values of p_u were added to define the edges of the transition between the tube-open and tube-collapsed states. As when obtaining the data for a control–space diagram, separate experiments were conducted for the cases of increasing and decreasing p_e. In each experiment, p_u was incremented or decremented in steps of 1 kPa, and p_e was then carefully adjusted at each step to attain the required value of $\bar{p}_{e1}$. The transition was thus eventually documented in terms of (in the case of increasing p_e) the last p_u-value at which the tube was open and the first p_u-value, 1 kPa higher, at which it was collapsed once the required $\bar{p}_{e1}$-value had been regained.

Thus, measurements of pressure and of flow rate constituted the main data of this experiment; in addition, the cross-sectional area of the tube throat was measured in one experiment, using the conductance catheter method as adapted for this application by McClurken (1978), with two separate single-electrode catheters (Bertram 1986). All experiments reported here were conducted with a low value of downstream flow resistance, that labelled R_2^l by Bertram *et al.* (1991).

3. RESULTS

Figure 1 shows the first stage in the construction of the control–space diagram for the case of decreasing p_e (which also implies decreasing $\bar{p}_{e2}$). Seven different values of p_u were investigated, and the results show all significant happenings along each of those seven descending paths. The symbols show that all the data obtained were of one of three types. Starting from the top of the line $p_u = 166$ kPa, for instance, initially the tube was in 'nf' mode

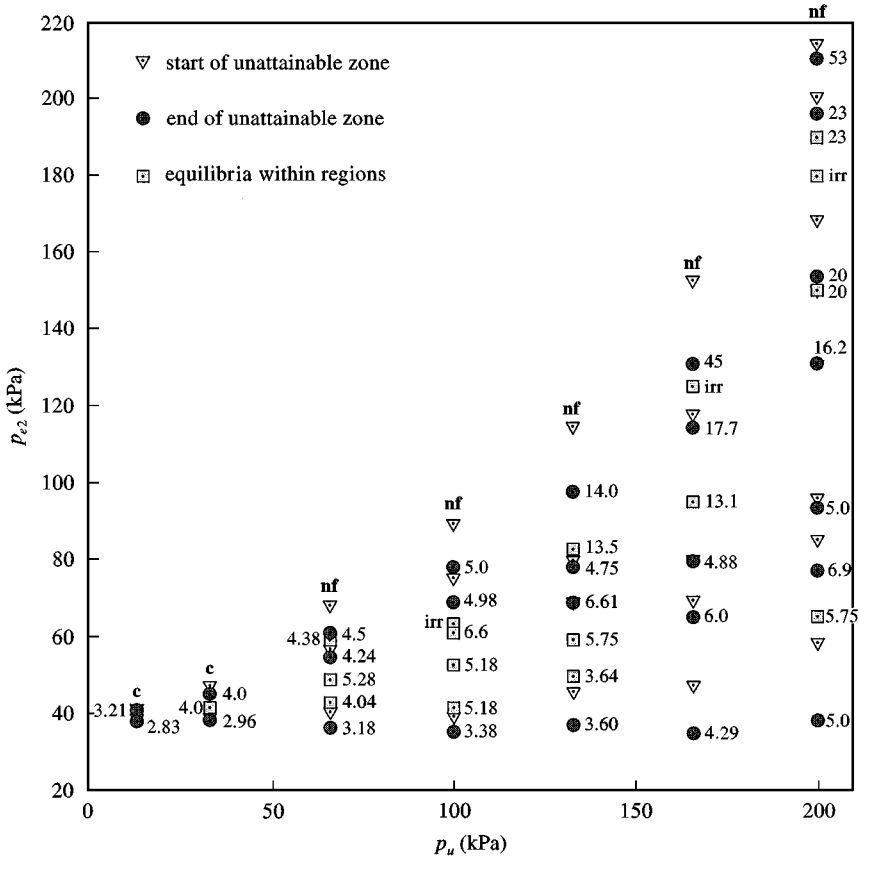

Figure 1. The raw data of the modified-control-space diagram consist of three different types of operating point as shown in the legend, plotted in terms of their $(p_u, \bar{p}_{e2})$-coordinates. Where applicable, symbols are accompanied by numbers giving the frequency of self-excited oscillation in Hz. All points on this diagram were approached by reduction of p_e, until either the required value of $\bar{p}_{e2}$ was reached or an unattainable zone was encountered. Seven different values of p_u were investigated, giving rise to the seven columns of data points. Each column was descended, starting at the top where either 'nf' or 'c' conditions prevailed; nf = small-amplitude noise-like fluctuations in p_2; c = steady flow with the tube collapsed. The final state in every case was steady flow again, but with the tube open.

(the mode abbreviations are explained in the next figure), then an unattainable zone was encountered (triangular symbol). The start of such a zone is of course an unstable point, analogous to the location of a cliff edge. The end point (circular symbol) is stable, and in this case is annotated as a 45 Hz self-excited oscillation. In general, such a zone separated each of a pair of contiguous modes from the other, except where the modal definitions are such that the transition was continuous and gradual. In the stable regions between unattainable zones, further operating points (square symbol) were investigated as necessary to complete the characterization, for instance in terms of frequency change. In the case of the line in question, the third symbol down is such a square, and is annotated to show that the periodic oscillation became irregular. Along this path, five unattainable zones were found altogether, separating six stable regions, in the last of which the tube was no longer collapsed, and steady flow occurred.

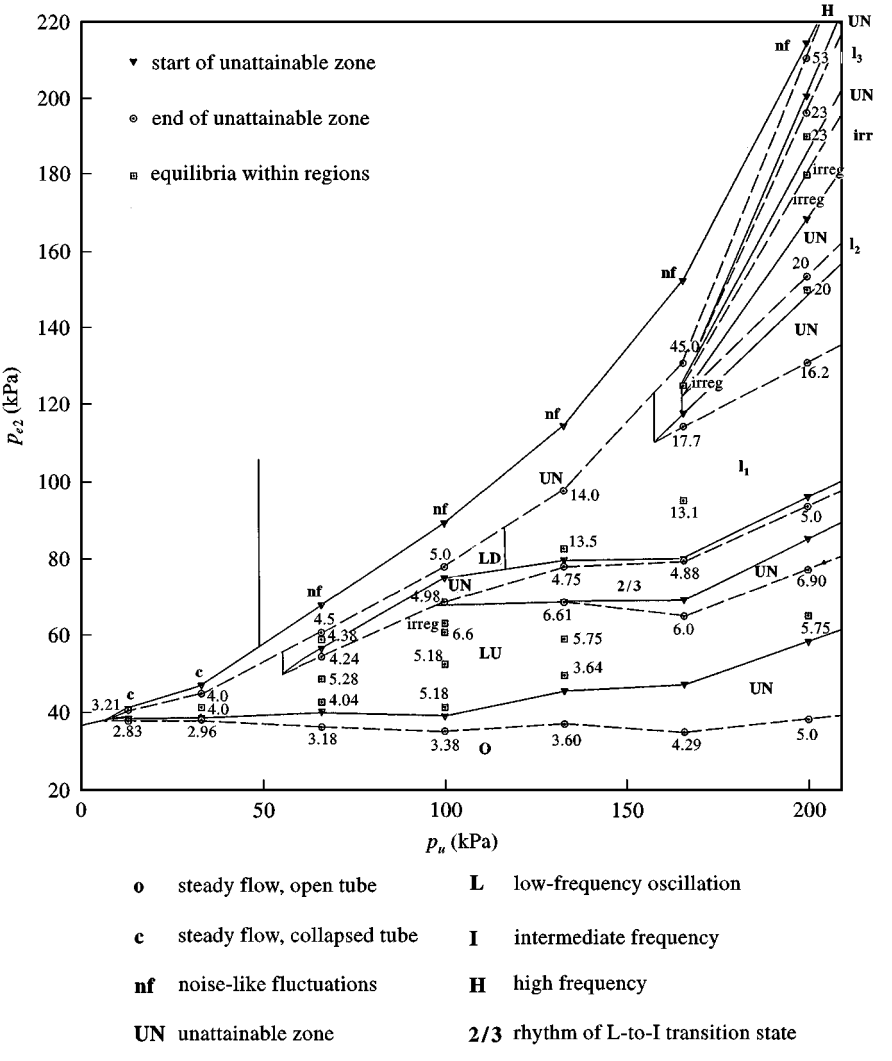

Figure 2. The control–space diagram is then constructed from the raw data in Figure 1 by construction of lines linking qualitatively similar happenings at different values of p_u and delineating closed regions of space within which a given type of behaviour or oscillation occurs. As far as possible, the process is conservative, involving straight-line interpolation and as little extrapolation as is needed to produce a diagram consistent with all known aspects of the tube behaviour. The key to the added mode-type abbreviations is given below the figure.

The next step is to interpret these data in terms of closed regions on the control–space diagram, some of which are recognizable from one value of p_u to the next, and some of which do not survive. Figure 2 shows the same data, now with the addition of lines delineating the boundaries of the regions, and (in bold) mode abbreviations. The boundary representing the end of an unattainable zone is marked as a dashed line, to indicate that its position depended on the dynamic qualities of the apparatus external to the collapsible tube, i.e. the parts of the flow circuit upstream of where p_1 was measured and downstream of where p_2 was measured, whereas the position of the start (solid line) was set by the instability of the

tube itself. [Our former practice (Bertram *et al.* 1991) of combining results for increasing and decreasing p_e therefore amounted to bounding unattainable zones by the solid line from each of the two diagrams we now construct.] The regions were constructed by inspection, according to principles of linear interpolation and least possible extrapolation. Where information was lacking, it was assumed, unless these principles suggested otherwise, that the change occurred at the midpoint of the intervening space. An example of this is the boundary between the LD and I_1 regions; at $p_u = 100\,\mathrm{kPa}$, only low-frequency oscillation of type LD was found, while at $p_u = 133\,\mathrm{kPa}$, only intermediate-frequency oscillation was seen at the equivalent region below the topmost unattainable zone.

In the final construction stage, the raw data were suppressed, leaving only the region boundaries and mode abbreviations; the result will be seen as the underlay in Figure 10 in the following. We have previously published extensive data in this form on how the dynamical behaviour of tubes of the type used here changes as their length and the downstream resistance are varied (Bertram *et al.* 1991), and as the distributed properties of the downstream apparatus are varied (Bertram & Butcher 1992). [Yamane & Orita (1994b) have published less complex diagrams showing the same main features in the same arrangement: in order of increasing p_e, initially no collapse, then regions of low- and higher-frequency oscillation, then audible noise present only at higher flow rates.] For the same tube as hitherto, Figure 3 shows the equivalent final construction of the control–space diagram when p_e increased. The diagram shows most of the same qualitative features as that in Figure 2, but the values of $\bar{p}_{e2}$ at which the unattainable-zone start and end points occurred differ, and there is considerable simplification of the dynamics at the highest values of p_u and $\bar{p}_{e2}$.

For this same situation of increasing p_e, Figure 4 shows the results of investigating behaviour at a series of constant values of $\bar{p}_{e1}$. As explained above, the axes for this experiment are $\bar{Q}$ and $\bar{p}_{12}$. All values of $\bar{p}_{e1}$ investigated, except the lowest (30 kPa), played flow limitation: the flow-rate $\bar{Q}$ was essentially independent of the pressure drop $\bar{p}_{12}$ where the curves are close to vertical. The range of $\bar{p}_{e1}$ values covered shows all three possibilities: at high $\bar{p}_{e1}$ the flow rate was flow-limited already at the lowest value of p_u used (13 kPa), and at the lowest $\bar{p}_{e1}$ it was not yet limited at the highest p_u-value available (200 kPa). Five intermediate values of $\bar{p}_{e1}$ in the range 31–35 kPa displayed a transition between steady flow at flow rates that depended sensitively on $\bar{p}_{12}$ through an as yet noncollapsed tube (points clustered in an almost horizontal band at the foot of the graph) and flow limitation. The start and end of the transition for these five curves are annotated with the p_u-values, showing that the transition occurred when p_u was increased by only 1 kPa.

The transition was stable in time; it is not a transient. However, it was unstable in the sense that, once p_u had been incremented past the last pre-transition value, the $\bar{p}_{e1}$-value pertaining to the curve being investigated was not regained until the transition was complete. Figure 5 shows in detail an example of what happened during the transition. The target value of $\bar{p}_{e1}$ is marked on the appropriate trace. As p_e was increased as slowly as possible, $\bar{p}_{e1}$ approached the target from below. But as the target got close, self-excited oscillation broke out, causing $\bar{p}_{e1}$ to fall away. Substantial further gradual increase in p_e was then necessary to compel $\bar{p}_{e1}$ to re-approach the target value, but before the target was attained, oscillation died away. Closer examination of this whole transient sequence reveals episodes of each of the types of oscillation expected from the $(p_u, \bar{p}_{e2})$-space regions traversed.

This last point can be made explicit by re-plotting the results of the constant-$\bar{p}_{e1}$ experiments on control–space axes. Since p_u, $\bar{p}_1$, $\bar{p}_2$ and p_e were measured for every operating point, this is straightforward. Figure 6 shows the data of Figure 4 overlaid on the control space of Figure 3. In this presentation, the points corresponding to parts of curves

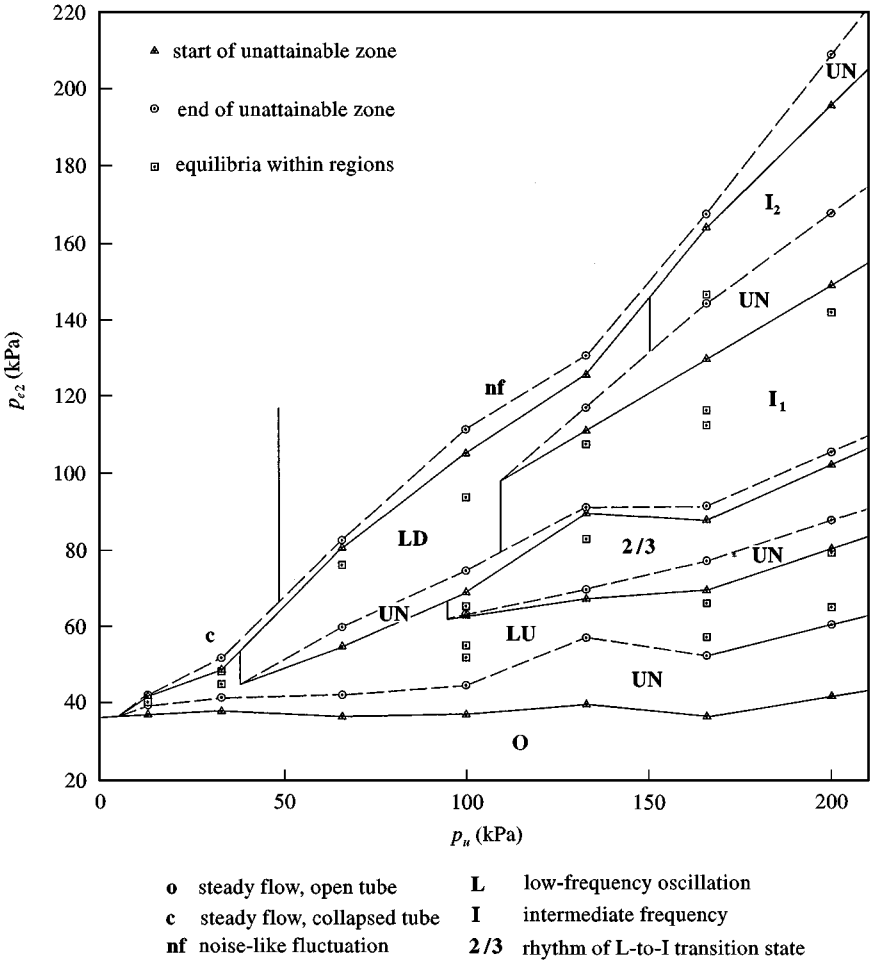

Figure 3. The corresponding control-space diagram to that shown in Figure 2, but for the case of increasing p_e. In this case, since the preceding stages have not been illustrated, the raw data points have been left on the diagram. All the boundaries occur in slightly different places from Figure 2, and some regions in Figure 2 at high $(p_u, \bar{p}_{e2})$-values are absent altogether.

where flow limitation occurred all lie above the highest unattainable zone. Absence of flow limitation is the case for the points lying below the lowest unattainable zone. (In fact, this group of points apparently strayed into the unattainable zone, an impossibility that is the result of slight misregistration between the two separate experiments compared here, and which will be discussed further below.) The five transitions are now seen as almost vertical lines between these two situations, spanning the several oscillation regions that were briefly visited in the example shown in Figure 5.

Simple calculation shows that the Reynolds number in these experiments based on undeformed tube diameter was approximately 100 times the flow rate in ml/s. Flow limitation as demonstrated in Figure 4 therefore occurred under turbulent flow conditions where the mechanism is expected to be choking (Griffiths 1969; Shapiro 1977a; Bertram 1995); at some critical point in the tube, the flow velocity $\bar{u} = \bar{Q}/A$, where A is cross-sectional area, becomes equal to the pressure wave velocity c. Downstream of that point the

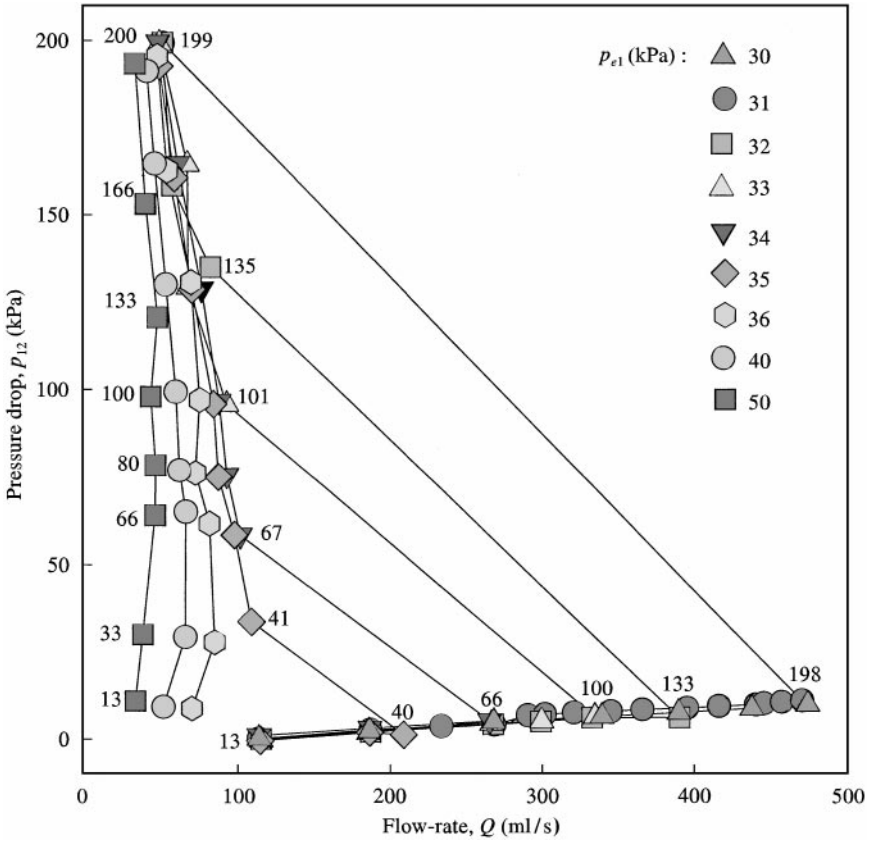

Figure 4. The results of investigating nine different constant-$\bar{p}_{e1}$ curves (see legend), plotting the results in terms of pressure drop down the tube and flow rate. Symbols are annotated with the value of p_u; eight different standard values of p_u were investigated (the annotations on the left of the curves), plus others as necessary to define the start and end of the transition to flow limitation to within 1 kPa, for those five curves which exhibited the transition. All points were approached by increasing p_e, until the required value of $\bar{p}_{e1}$ was reached.

flow is supercritical ($\bar{u} > c$) and the tube is collapsed, until the proximity of the downstream boundary condition on pressure and area forces a return to subcritical flow via a shock-like elastic jump. In the tubes used here, the locations of the hypothesized passage to and from the supercritical state were close together; the collapsed throat of the tube was typically short. By measuring the cross-sectional area of the tube, it is possible to estimate both $\bar{u}$ and c, the latter on the basis of the relation $c^2 = (A/\rho)\,(\mathrm{d}p/\mathrm{d}A)$ derived by Young (1808). The catheter electrodes were located at the centre of the collapsed throat, where if the above-hypothesized conditions pertain, $\bar{u} > c$.

Figure 7 shows the data from another experiment with increasing p_e, similar to but not identical to Figure 4, in which A was measured. The symbols in Figure 7 are annotated with the calculated values of $\bar{u}$ for every operating point, both those in the putative choking region and those where choking is not expected. The values for points in the flow-limitation condition ranged between 2·16 and 6·41 m/s, if the points recorded with $p_u = 13$ kPa be excluded on the basis that the existence of flow limitation is not proven here. Bertram (1987) measured the no-flow $A(p)$ for the same tubing, at various distances from the end constraint.

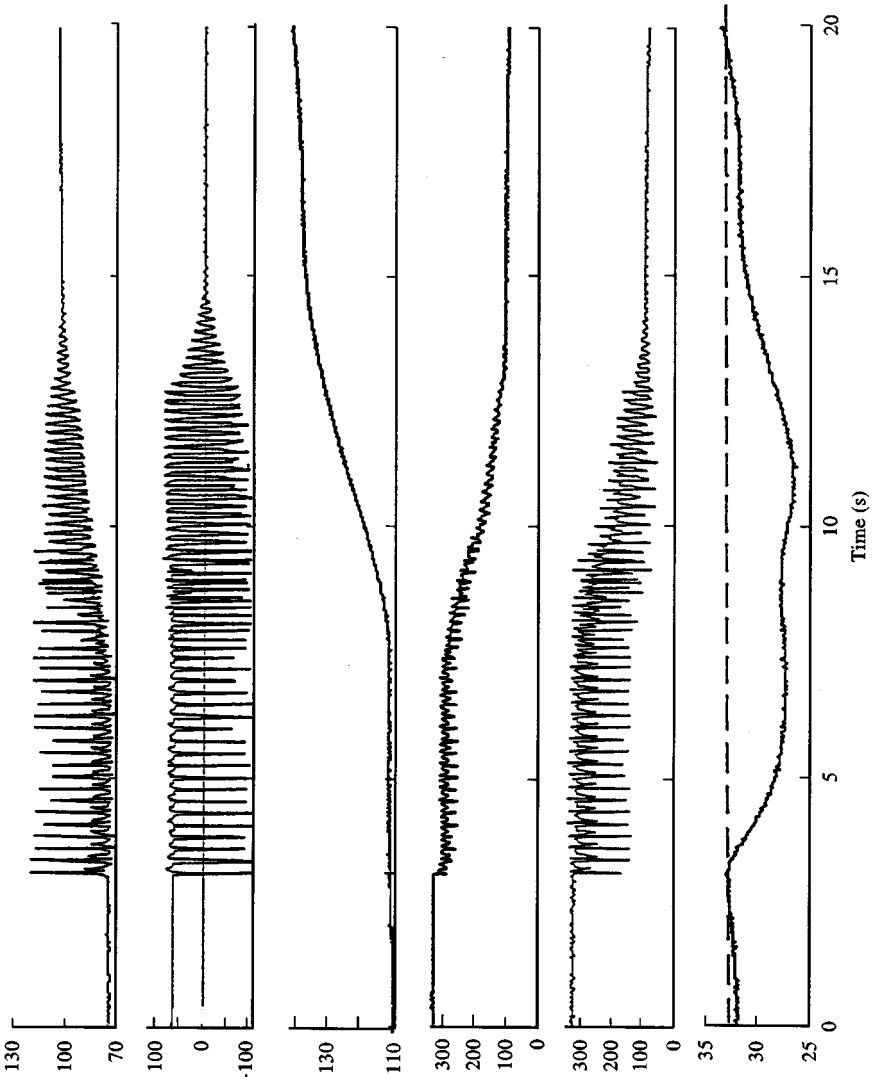

Figure 5. Events occurring when, with $p_u = 101$ kPa, the transition to flow limitation was crossed on the constant-$\bar{p}_{e1}$ curve for $\bar{p}_{e1} = 33$ kPa with p_e increasing. According to the control-space diagram (see Figure 3), which is drawn up under carefully adjusted static conditions, the transition crosses regions of LU, 2/3 and LD oscillation. The recording shown here, when p_e was varying, actually includes episodes of LU (gradually increasing in frequency), a 2/3-then-1/3 rhythm related to the expected 2/3, and a less-than-fully-periodic LD oscillation, before the amplitude decays, leaving the much smaller nf mode. This sequence of events is the middle one of the five transitions shown in Figure 4.

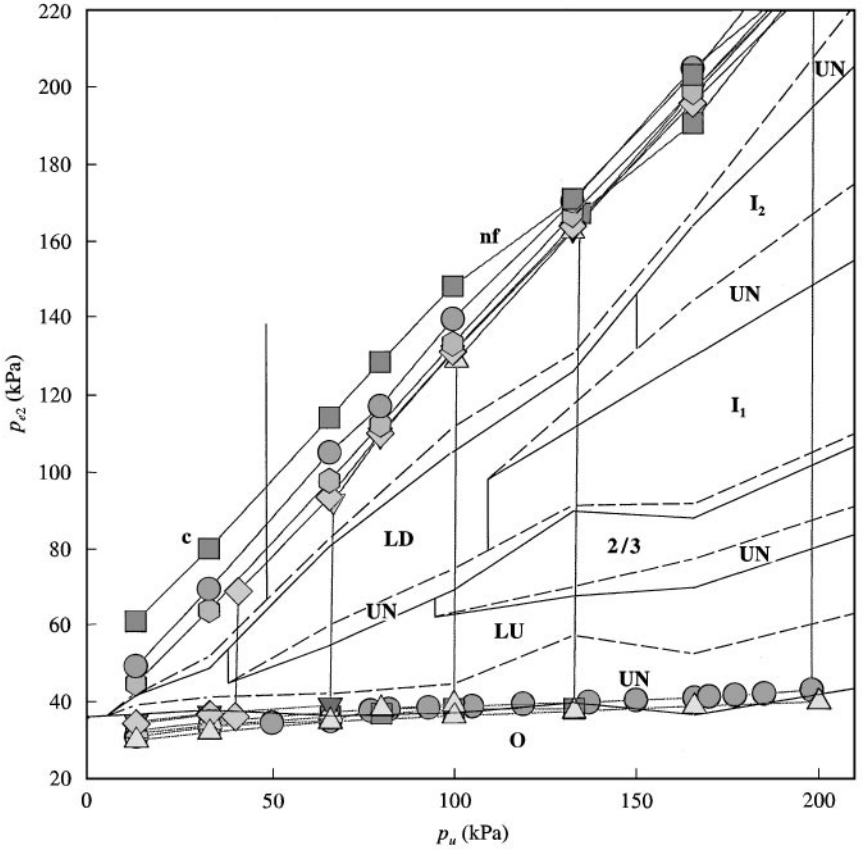

Figure 6. The control-space diagram of Figure 3, with the constant-$\bar{p}_{e1}$ curves of Figure 4 overlaid using their appropriate $(p_u, \bar{p}_{e2})$-coordinates. What were in Figure 4 the operating points having consistently low $\bar{p}_{12}$ are now the group at low $\bar{p}_{e2}$; the flow-limiting operating points now occupy the nf region. Transition to flow limitation forms the five almost-vertical lines joining these two groups.

The derived minimum values of c (during partial collapse) depended systematically on end proximity, ranging down to around 1·5 m/s far from the constraint but increasing to around 2·4 m/s at 18 mm from the end and 4·0 m/s at 9 mm, for a tube having the same thickness and longitudinal tension (fig. 10a, that paper) as the one used here. Bertram & Raymond (1991) made direct measurements of wave velocity during flow-induced oscillation, using high-frequency wavepackets. By an indirect process the low-frequency wavespeed appropriate to the oscillation was estimated to be between 2·5 m/s at $A = 0{\cdot}4$ and 4 m/s at $A = 0{\cdot}7$ (fig. 6, that paper). Thus, the range of $\bar{u}$-values calculated here spans completely and also exceeds the likely range of c. Although the argument is obviously weakened by the fact that c and $\bar{u}$ were not measured in the same circumstance, this comparison suggests that supercritical flow could have existed at all operating points where flow limitation occurred.

In view of the extent to which self-excited oscillation and flow limitation by the wave-speed mechanism have sometimes appeared from the literature to be associated phenomena, the most striking aspect of the results shown in Figures 4 and 7 was that none of the operating points in the group showing flow limitation exhibited large-amplitude or periodic oscillation. All lay in the control-space region labelled 'nf', indicating small-amplitude noise-like (broadband and aperiodic) fluctuations, principally of p_2.

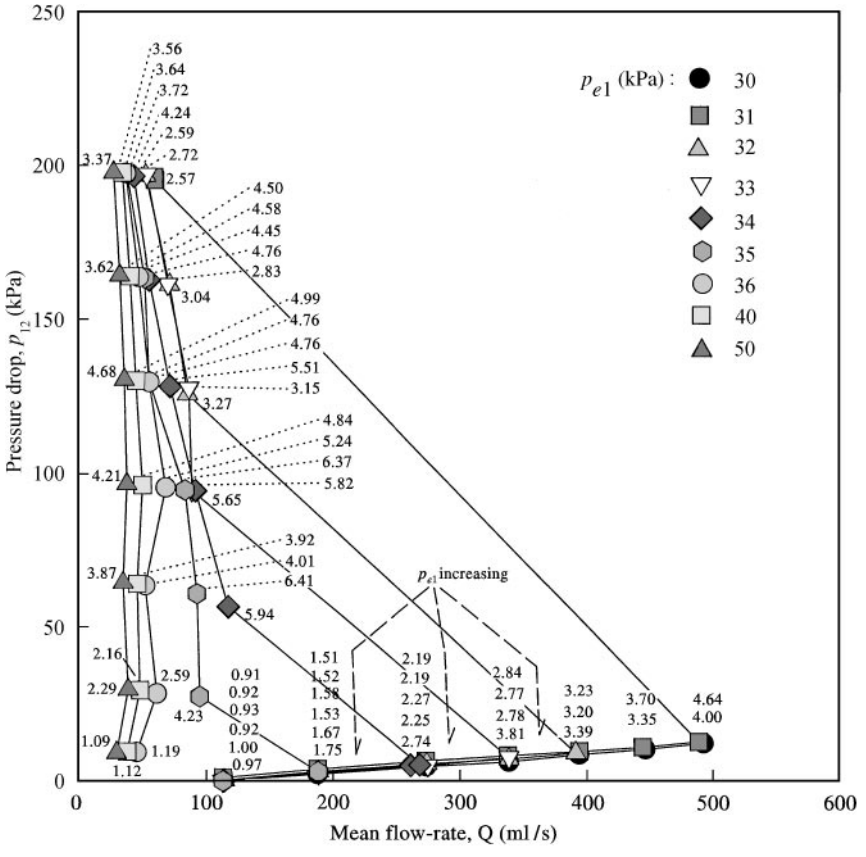

Figure 7. The results of an experiment similar to that shown in Figure 4, but in which the cross-sectional area of the tube throat was measured, allowing calculation of $\bar{Q}/A$, the fluid velocity averaged over the cross-section appropriate to 1-D theory, for every operating point, as shown by numerical annotations.

Turning to the situation of decreasing p_e, a similar absence of large-amplitude or periodic oscillation was found over most, but in this case not all, of the operating points showing flow limitation. The results for decreasing p_e are shown in Figure 8. It is seen that the range of $\bar{p}_{e1}$-values needed to cover all three behaviour possibilities (always flow-limited, never flow-limited, or with transition from flow limitation) does not overlap at all the equivalent range for increasing p_e. Transition was found at seven $\bar{p}_{e1}$-values, from 10 to 22 kPa. Some or all of the flow-limited operating points on the curves for $\bar{p}_{e1} = 10$ to 16 kPa exhibited moderately large-amplitude oscillations, which were either aperiodic (annotated "irreg") or periodic with a frequency of 22 Hz.

The symbol legend for Figure 8 shows, in addition to the final or target value of $\bar{p}_{e1}$ for each curve, an initial value for each symbol (e.g. "from 18"). At every operating point, first p_u was set, then p_e was carefully adjusted such that $\bar{p}_{e1}$ first reached the initial value, then descended onto the target value. (Since $\bar{p}_{e1}$ was monotonic with p_e except in the transition, and since the current value of $\bar{p}_{e1}$ was continuously displayed using a multimeter to subtract the low-pass filtered p_1-signal from the similarly calibrated p_e-signal, this process was not as difficult as may appear.) The importance of the initial value is that a second, quite different behaviour could be obtained for certain target $\bar{p}_{e1}$-values, if the initial value of $\bar{p}_{e1}$ was only

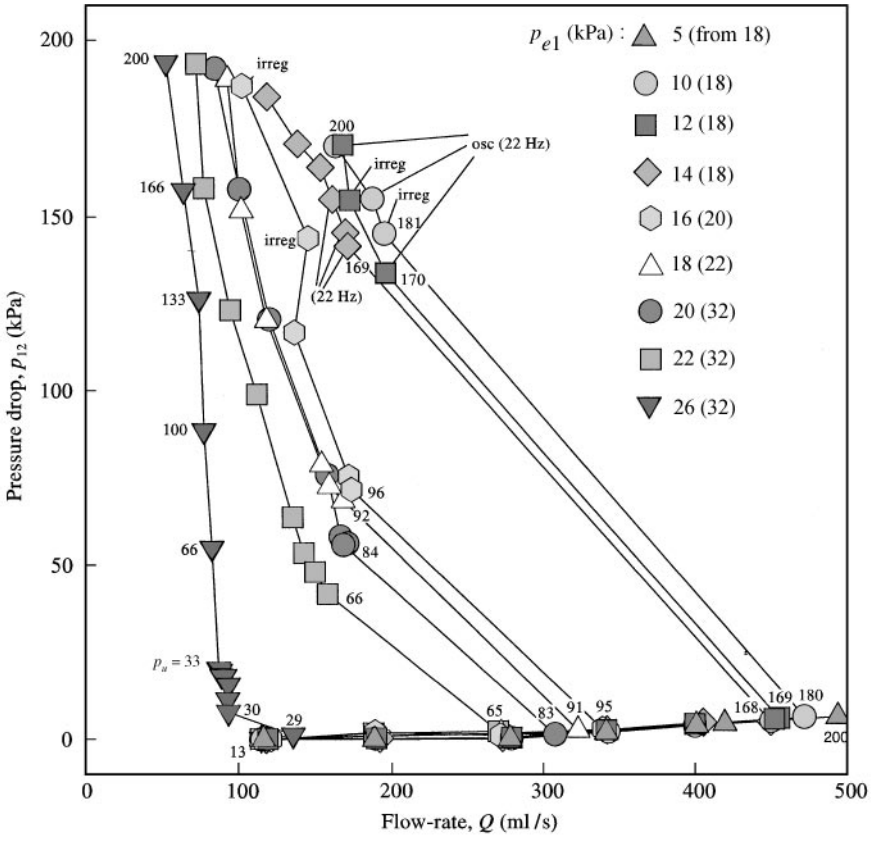

Figure 8. The results of investigating nine different constant-$\bar{p}_{e1}$ curves (see legend), plotting the results in terms of pressure drop down the tube and flow rate, as in Figure 4, but now reducing p_e until the required value of $\bar{p}_{e1}$ was reached. Most of the symbol annotations relate to the value of p_u as in Figure 4; in addition, the group of oscillatory operating points are indicated by the annotations 'irreg' or '(22 Hz)'. The legend shows both the target $\bar{p}_{e1}$-value and (in parentheses) the starting value.

just above the target value. Figure 9 shows this second behaviour, observed for target values of $\bar{p}_{e1}$ in the range 14–26 kPa. The initial value of $\bar{p}_{e1}$ is now such that the tube was initially open (not collapsed), and remained so as the target $\bar{p}_{e1}$ was attained. Note that the vertical scale on Figure 9 is unchanged from that of Figure 8, to show that these five curves all belong to the point cluster in the almost horizontal band at the foot of Figure 8.

As for the case of increasing p_e, the results shown in Figure 8 can be re-plotted to advantage on the control-space diagram of Figure 2. The result of so doing is shown as Figure 10. There are broad similarities with the equivalent overlay in Figure 6. Differences include the increased vertical ($\bar{p}_{e2}$) separation of the individual overlaid curves in Figure 10, both when the tube was open and when flow limitation was occurring, and of course the existence of operating points that combined flow limitation with irregular or 22 Hz oscillation. These points, distinguished in Figure 10 from steady-flow operating points by symbol shading, straddle regions which during the control-space experiment were found to be periodically oscillatory at either intermediate (I_3 : 23 Hz) or high (H : 45–53 Hz) frequencies—see Figure 2. They also appear to overlay parts of the nf region and the topmost

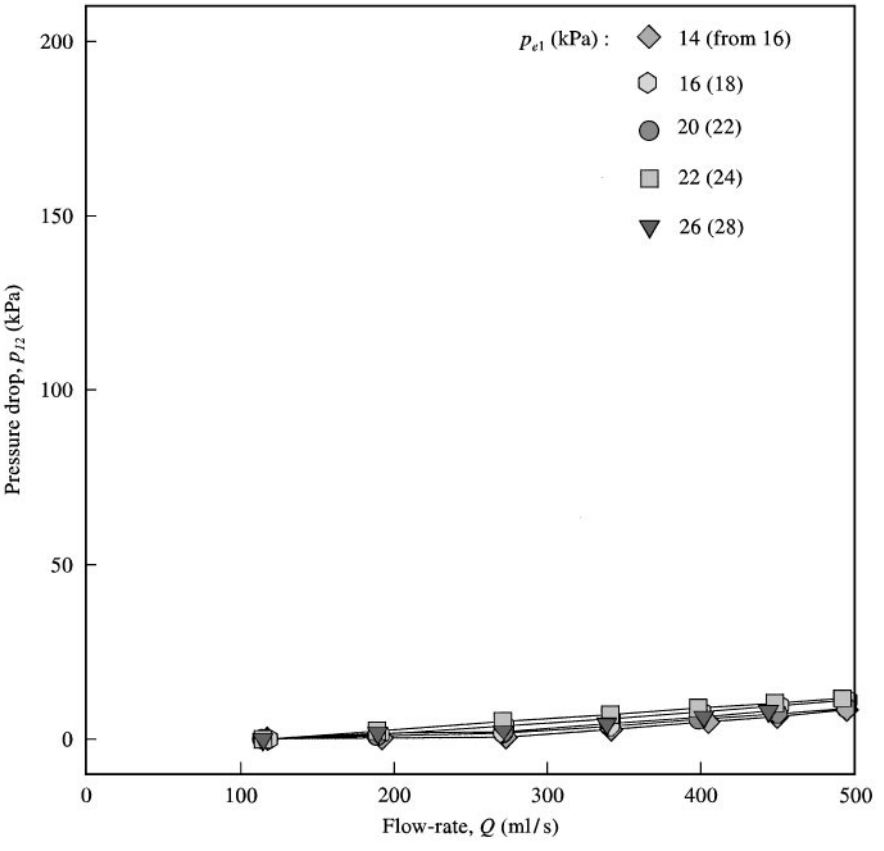

Figure 9. On the same scale as Figure 8 are shown constant-$\bar{p}_{e1}$ curves where the target value of $\bar{p}_{e1}$ was reached by reducing p_e so that $\bar{p}_{e1}$ declined from a starting value slightly greater than the target (shown in parentheses in the legend) at which the tube was not yet collapsed. When these same target values of $\bar{p}_{e1}$ were investigated starting from higher $\bar{p}_{e1}$-values at which the tube was initially collapsed, the result was flow limitation (as shown in Figure 8) which is absent here.

unattainable region, but do not overlay the region of irregular or aperiodic oscillation below the I_3-region.

4. DISCUSSION

Probably the most important result to emerge from this work is the finding that flow limitation and large-amplitude self-excited oscillation are not always coupled; flow limitation can occur without incurring oscillation, in a situation where, on the basis of both Reynolds number and comparison of flow and wavespeeds, flow limitation is undoubtedly by the wavespeed mechanism. How generic is this behaviour? Would essentially the same picture occur at larger values of downstream resistance, for example? We have investigated previously how dynamical behaviour depends on downstream resistance (Bertram *et al.* 1991). Increased resistance led to a reduced tendency for oscillation. The resistance value used here was the smallest of the three used then. Thus, we believe that larger resistance would further inhibit oscillation, and to that extent our finding is generic. We can but speculate about what would happen if the resistance downstream were reduced below the

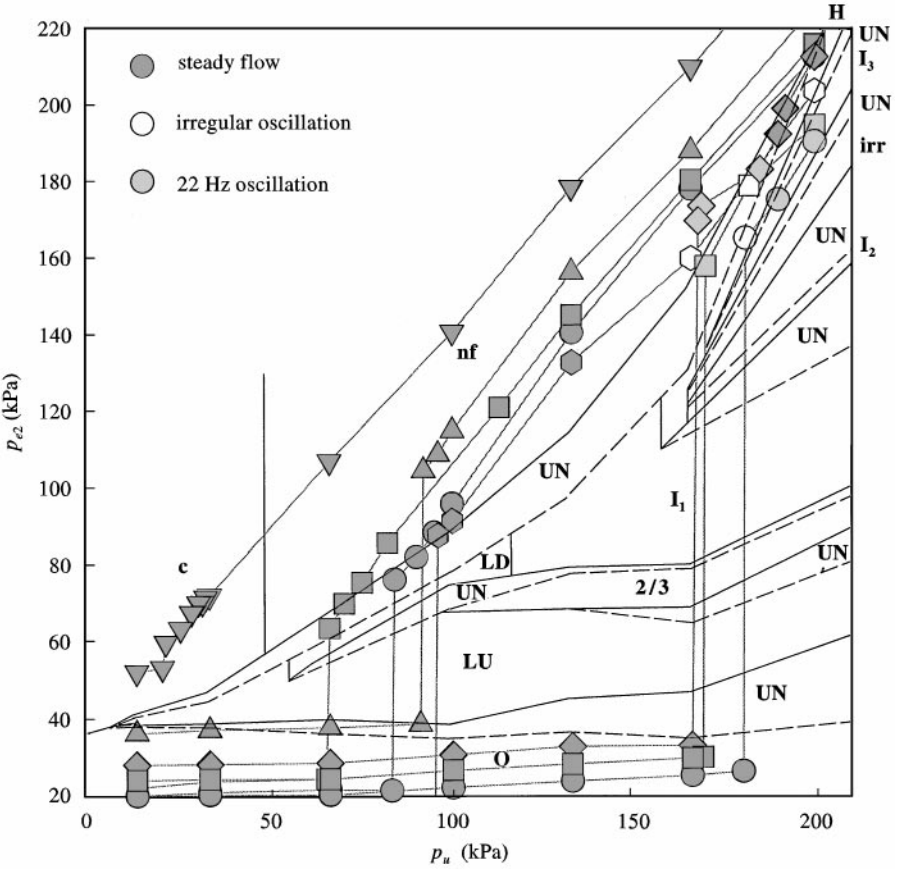

Figure 10. The control-space diagram of Figure 2, with the constant-$\bar{p}_{e1}$ curves of Figure 8 overlaid using their appropriate (p_u, $\bar{p}_{e2}$) -coordinates. Symbol shading has been reorganized so that the group of oscillatory points which was annotated as such in Figure 8 can be identified by symbol shading here.

value used here (by removing apparatus components). It is possible that oscillation would then dominate. However, this would be a finding of lesser importance than what we have shown, namely that, self-excited oscillation is not a *necessary* concomitant of wavespeed-mediated flow limitation.

The comparison of separate experiments represented by overlaying constant-$\bar{p}_{e1}$ curves on control-space constructions as in Figures 6 and 10 is necessarily an inexact process. The major source of error is likely to have been drift in pressure transducer calibrations. In general, the process of subtracting two measurements from each other, as in the derivation of $\bar{p}_{12}$, $\bar{p}_{e1}$ or $\bar{p}_{e2}$, always multiplies the relative effect of initially small errors in calibration. Use of analogue (electronic circuit) filters adds another error source, in that the indicated value of $\bar{p}_1$, say, may not be exactly the true mean of $\bar{p}_1$, despite careful prior adjustment using constant-voltage inputs. Although this problem can be circumvented by averaging in software after digital recording, no such strategy was available to us in the context of experiments where a given value of $\bar{p}_{e1}$ or $\bar{p}_{e2}$ was set by adjusting p_e. We had a particular problem with the measurement of p_2, ultimately because of the violence of self-excited oscillations in the thick-walled tubing used here. Downstream of the tube throat, the pressure during an oscillation cycle transiently becomes low enough to cause cavitation. In

special experiments at high digitisation rates (She 1996), we have recorded evidence of cavitation in the form of extremely short-lived pressure transients. We have never recorded transient pressure great enough to exceed the normal range of our pressure transducers, but it would appear from the failure of successive p_2 transducers that they occur. For that reason we have been forced to adopt the use of p_2 transducers having an excessively wide range. The penalty for so doing is that an acceptable overall drift specification becomes an unpleasantly large drift in the context of use to record pressures over only a small part of the transducer range. Despite transducer recalibration as frequently as possible, part of this drift undoubtedly found its way into the results. Besides error in pressure measurement, other factors that may have changed subtly between experiments include the temperature and hence viscosity of the flowing fluid, and inevitably the 'age' of the tube itself in terms of oscillation cycles. Short of implementing an actively controlled refrigeration system it is difficult to avoid slight variations in temperature as the recirculation-system pumps add heat, despite taking data only when the liquid temperature was within a narrow acceptable range. For all of the above reasons, the overlays shown in Figures 6 and 10 should be interpreted cautiously in respect of fine detail.

Despite this shortcoming, the re-plotting of the constant-$\bar{p}_{e1}$ curves on control space is a valuable tool for interpreting the flow limitation results, and in particular for understanding what is happening during the complex transition shown in Figure 5. We believe that this is the first time that an analysis and an explanation of the events occurring during the transition from steady flow through a non-collapsed tube to the flow-limited condition has been offered. Although previous workers have recorded the fact that this transition involves a notch or small portion of curve which has a distinct negative slope (Brecher 1952; Bonis 1979), it seems that the transition is much more prominent in Figure 4,7 and 8, relative to the range of flow rates seen during flow limitation.

The small range of flow-limited flow rates, relative also to the systematic and non-systematic variations from one operating point to the next on a given curve, means that it cannot be determined with confidence by inspection of Figure 4 or Figure 8 whether there was a monotonic relation between the flow-limited flow rate (call it Q_c) and $\bar{p}_{e1}$. To answer this question, the Q_c-value at $p_u = 200$ kPa on each curve was plotted against $\bar{p}_{e1}$, for both increasing and decreasing p_e, as shown in Figure 11. The choice of $p_u = 200$ kPa was because this, the maximum value investigated, the only p_u-value for which a point on the flow-limited part of the constant-$\bar{p}_{e1}$ curve is available for all constant-$\bar{p}_{e1}$ curves. The result shows that within each of the two segments of curve plotted in Figure 11, there is indeed a monotonic relation between Q_c and $\bar{p}_{e1}$. However, the two segments do not appear to be different parts of one and the same overall curve, suggesting that there was *not* a single underlying relation between Q_c and $\bar{p}_{e1}$, irrespective of whether p_e was increasing or decreasing. Instead, Figure 11 suggests that Q_c does not depend uniquely on $\bar{p}_{e1}$, because it also depends on the direction of approach to the $\bar{p}_{e1}$-value. Although there is a lack of overlap between the increasing- and decreasing-$\bar{p}_{e1}$ ranges over which flow limitation was observed, as noted above, there is already visible at around $Q_c = 60$ ml/s a small range of Q_c-values which were achieved by two quite different values of $\bar{p}_{e1}$, depending on whether the target $\bar{p}_{e1}$-value was approached from above or from below. Kamm *et al.* (1993) have previously demonstrated nonunique dependence of Q_c on $\bar{p}_{e1}$ for air-flow through tubes of tapering wall thickness (becoming stiffer downstream)

A degree of 'negative effort dependence' is also manifest in Figures 4 and 8. This term, which is borrowed from pulmonary physiology, denotes in this context that when flow limitation was occurring, $\bar{Q}$ decreased as $\bar{p}_{12}$ increased. For increasing p_e (Figure 4) the extent of this tendency apparently depended on $\bar{p}_{e1}$ in a nonlinear way, being greatest at the highest values of $\bar{p}_{e1}$ which manifested transition (34–35 kPa), and less for both higher and

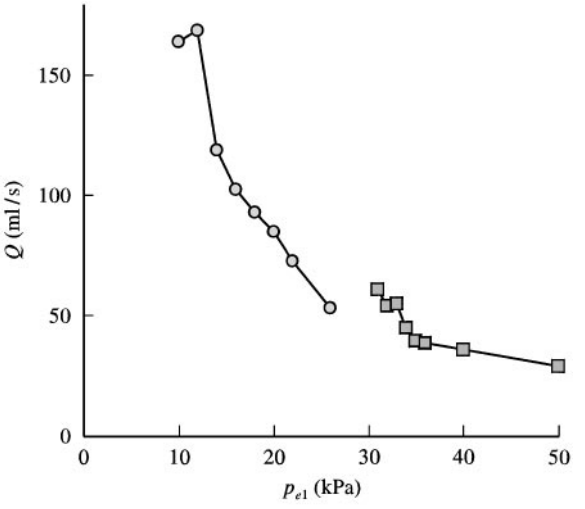

Figure 11. Data from Figures 7 and 8 are here combined to show how $\bar{Q}$ under flow-limited conditions varies with $\bar{p}_{e1}$, for both increasing p_e(□) and reducing p_e (○) conditions. All points relate to the condition $p_u = 200$ kPa, which provides the maximum number of flow-limited data points.

lower values. For decreasing p_e (Figure 8), an overall trend is less clear; the batch of points where irregular or periodic oscillation occurred seem to change the pattern. All constant-$\bar{p}_{e1}$ curves in Figure 8 showing flow limitation show considerable negative effort dependence, although it seems inevitable that less dependence would have occurred at higher values of $\bar{p}_{e1}$ than were investigated. The extent to which Q_c depends on $\bar{p}_{e1}$ is thus itself dependent on the range of p_u-values investigated; Q_c changes less with $\bar{p}_{e1}$ as p_u increases.

Many others have compared $\bar{u}$ and c as attempted for the data here, e.g. Brower & Scholten (1975), Elliot & Dawson (1979), Kececioglu *et al.* (1981), Yamane & Orita (1994a). The comparison here is much too crude to count as a significant contribution to the theoretical (Grotberg & Reiss 1984; Walsh *et al.* 1991) and experimental (Bertram & Raymond 1991; Yamane & Orita 1992) debate about whether or which types of self-excited oscillation can occur in the absence of choking. Rather it indicates simply that supercritical flow probably occurred whenever the pressure-drop/flow-rate relation showed that the flow rate was limited. For the purposes of this paper, the two conditions, the one mechanistic and only indirectly and partially supported by experimental evidence, the other a direct and unequivocal demonstration, can be taken as having coincided.

Because of the extent to which the flow rate was reduced during the transition on the curves showing flow limitation (Figures 4, 7 and 8), we have here adopted perhaps a more restricted definition of flow limitation than might be assumed by physiologists; we take flow limitation to have existed from the end of the transition when p_e increased, and as far as the beginning of the transition when p_e decreased. Our definition thus conforms with the visible demonstration on these curves of a largely constant flow rate, except for the negative effort dependence, once flow limitation occurred. The other possibility is that one regards flow limitation as starting at the point where flow rate no longer increases with the pressure drop, i.e. at the start of the transition when p_e increases. This distinction has mechanistic consequences, because our definition implies that the event causing the transition to begin is not choking itself. For an explanation we turn again to the control-space diagram on which the constant-$\bar{p}_{e1}$ curves are overlaid (Figure 6). Referring to those curves which execute the transition, and starting at the low-p_u, low-$\bar{p}_{e2}$ end, it is seen that the path of each curve is

almost parallel to the lower margin of the first unattainable zone, but gradually draws closer to the edge. As before, no exact detail can be read into this overlay of two different experiments, but the overall trend is clear. When the edge is reached, the operating point must pass to the far side of the unattainable zone and into regions of oscillation; the transition has begun. The loss of stability of the open tube occurs because a topological fold has been reached (Bertram *et al.* 1991; Bertram 1995) in what at zero flow rate would be the tube law relating transmural pressure and area. The transition itself involves large changes in flow rate; it is impossible to argue that flow rate is independent of pressure drop until the end of the process leaves the operating point in the nf-region. Beyond defining the (p_u, $\bar{p}_{e2}$)-coordinates for nf behaviour, the control-space diagram is mute about what happens in this region, but these experiments make clear that flow-rate limitation occurs and, on the grounds both of the high Reynolds number and of the rough parity of $\bar{u}$ and c established above, that choking almost certainly is the cause. One may speculate that the regions of large-amplitude oscillation traversed during the transition are also regions where flow-rate limitation by choking occurred transiently rather than continuously, only during the most collapsed phase of each cycle, but the experiments provide no direct evidence to support this idea. However, the experiments do appear to show that oscillation can disturb flow limitation; comparison of Figures 7 and 8 suggests that the occurrence of both aperiodic and periodic oscillation perturbed the shape of those parts of the curves in Figure 8, changing slightly the flow-limited flow rate.

Gavriely *et al.* (1989) concluded that flow limitation is associated with flutter, rather than lower-frequency oscillations, and that flow limitation is a necessary but not sufficient precondition for the generation of flutter in tubes. The equivalent result here is that flow limitation is associated with one of three conditions: usually the small-amplitude "nf" mode, but under certain circumstances of decreasing p_e, either a larger-amplitude aperiodic mode ("irreg") or an intermediate-frequency periodic mode of 22 Hz. The "nf" mode has been illustrated in our previously published papers, both as a time series (fig. 5, Bertram 1986a) and as a spectrum (fig. 5b, Bertram *et al.* 1991), and time series for larger-amplitude aperiodic oscillations were given by Bertram *et al.* (1991, fig. 1.). There are many differences between our experiments and those of Gavriely *et al.*, the most important of which is probably that most of their reported results pertain to a latex tube of similar wall-thickness and internal diameter of 6.5 mm conveying air, in which they observed flutter in the frequency range 280–720 Hz. They also used a tube which was rather similar to ours: Silastic of inside diameter 11·8 mm and wall thickness 1·9 mm conveying water; for this they showed spectra with a sharp peak at about 160–170 Hz. Broadly the results here tend to support their findings, if what we have characterized as 'nf' be identified with flutter in their experiments. Quantitatively, the 22 Hz mode here has no counterpart in their results, but we have, in the context of pressure-drop limitation experiments, previously recorded flutter-like oscillations at 100–200 Hz (Bertram *et al.* 1990) and occasionally as much as 600 Hz (Bertram 1986b) from similar tubes to that used here. Our results broadly confirm their suggestion that the wheezing associated with pulmonary expiratory flow limitation is not likely to be analogous to the large-amplitude, low-frequency oscillations which are so prominent in the laboratory-bench experiments on collapsible tubes.

However, it remains possible to visualize a mechanism whereby oscillations analogous to these large-amplitude ones may yet be involved in the sounds produced during such forced vital capacity manoeuvres. In the context of the present bench experiments, we find that the transition to or from the flow-limited state is where these oscillations reside. Parameter differences, including aqueous flow, enforce caution in applying this result to pulmonary airway collapse. However, in the airways there is a spatial and temporal variation of geometrical and mechanical properties which causes the site of flow limitation to move

progressively upstream during a forced expiration. Thus, there is always a site just downstream of the current flow-limiting position which is no longer collapsed, having presumably crossed some transition similar to that measured in the tube experiments. Particularly at the beginning of a forced expiration, the airways in question are the large and relatively stiff ones which are closer in properties to the tube here, in which the transition formed a major part of the flow-limitation curves. It is therefore suggested that a component of the audible wheezing at the start of a maximal forced expiration manoeuvre could be caused by the airway equivalent of large-amplitude oscillation, occurring in those airway segments which are being left downstream by the upstream-moving flow-limitation front. For each site in the airways, the oscillation would be a transient, but continuous sound production could result as the trailing edge of the front moves deeper into the lung. On this basis, while it seems that the large-amplitude modes of collapsible-tube oscillation are not as intimately associated with flow limitation as has sometimes been supposed, it may be that these 'traditional' collapsible-tube modes are still involved in lung wheezing.

5. CONCLUSIONS

Flow limitation was demonstrated to occur in thick-walled collapsible tubes, by keeping the transmural pressure at the upstream end constant. Negative effort dependence was exhibited, and the transition from noncollapse to the flow-limited state involved a complex transition characterized by a major reduction in the flow rate and passage through one or more modes of large-amplitude self-excited oscillation. When transmural pressure was set by increasing external pressure, flow limitation was never accompanied by large-amplitude or periodic oscillation. Hysteresis in both the tube mechanical properties and the system dynamics as a whole [noted also by Yamane & Orita (1994b)] caused somewhat different outcomes when transmural pressure was set by decreasing external pressure. Under these conditions, flow limitation with large pressure drop along the tube and small values of upstream transmural pressure was accompanied by aperiodic or periodic oscillation of significant amplitude. Also under these conditions, it was possible to obtain either flow limitation or absence of collapse at the *same* upstream transmural pressure, depending on whether external pressure was decreased from an initial value sufficient to cause collapse or not. This finding, involving the transmural pressure history, represents a qualification of the generally accepted notion that the upstream transmural pressure uniquely controls the flow rate in flow limitation. For a given direction of external pressure variation, the flow-limited flow rate was monotonically and inversely related to the upstream transmural pressure. However, a more serious departure from the notion of unique dependence on upstream transmural pressure was also caused by the hysteresis: the same flow-limited flow rate could be achieved by two different values of the upstream transmural pressure, depending on how the external pressure was varied to achieve these values. We believe that this is the first time that such nonunique dependence has been demonstrated for aqueous flow and for uniform tubes. The complexity of the transition to and from the flow-limited state was analysed and explained to advantage by use of a modified control-space diagram on which all oscillatory, steady or divergent collapsible-tube modes appear as closed regions.

ACKNOWLEDGEMENTS

RJC was supported by an Australian Research Council grant to CDB. Experimental facilities used were available as a result of several successive past Australian Research Council grants. The recirculation system was funded through a past University of New

South Wales development grant. CDB is grateful to Professor R. D. Kamm of the Massachusetts Institute of Technology for advice.

References

Bertram, C. D. 1986a Unstable equilibrium behaviour in collapsible tubes. *Journal of Biomechanics* **19,** 61–69.

Bertram, C. D. 1986b Collapsed tube instability during flow: effects of tube length. *Proceedings of the Fifth International Conference on Mechanics in Medicine & Biology*, Bologna, Italy, 1–5 July, pp. 91–94.

Bertram, C. D. 1987 The effects of wall thickness, axial strain and end proximity on the pressure-area relation of collapsible tubes. *Journal of Biomechanics* **20,** 863–876.

Bertram, C. D. 1995 The dynamics of collapsible tubes. In *Biological Fluid Dynamics* (eds C. P. Ellington & T. J. Pedley), pp. 253–264. Cambridge, U.K. : Company of Biologists Ltd.

Bertram, C. D. & Butcher, K. S. A. 1992 A collapsible-tube oscillator is not readily enslaved to an external resonator. *Journal of Fluids and Structures* **6,** 163–180.

Bertram, C. D. & Raymond, C. J. 1991 Measurements of wave speed and compliance in a collapsible tube during self-excited oscillations: a test of the choking hypothesis. *Medical and Biological Engineering and Computing* **29,** 493–500.

Bertram, C. D., Raymond, C. J. & Pedley, T. J. 1990 Mapping of instabilities for flow through collapsed tubes of differing length. *Journal of Fluids and Structures* **4,** 125–153.

Bertram, C. D., Raymond, C. J. & Pedley, T. J. 1991 Application of dynamical system concepts to the analysis of self-excited oscillations of a collapsible tube conveying a flow. *Journal of Fluids and Structures* **5,** 391–426.

Bonis, M. 1979 Ecoulement visqueux permanent dans un tube collabable elliptique. Thèse de Doctoral d'Etat, Université de Technologie de Compiègne, France.

Brecher, G. A. 1952 Mechanism of venous flow under different degrees of aspiration. *American Journal of Physiology* **169,** 423–433.

Brower, R. W. & Scholten, C. 1975 Experimental evidence on the mechanism for the instability of flow in collapsible vessels. *Medical and Biological Engineering* **13,** 839–845.

Elliott, E. A. & Dawson, S. V. 1979 Fluid velocity greater than wavespeed and the transition from supercritical to subcritical flow in elastic tubes. *Medical and Biological Engineering and Computing* **17,** 192–198.

Fry, D. L., Ebert, R. V., Stead, W. W. & Brown, C. C. 1954 The mechanics of pulmonary ventilation in normal subjects and in patients with emphysema. *American Journal of Medicine* **16,** 80–97.

Gavriely, N., Shee, T. R., Cugell, D. W. & Grotberg, J. B. 1989 Flutter in flow-limited collapsible tubes: a mechanism for generation of wheezes. *Journal of Applied Physiology* **66,** 2251–2261.

Griffiths, D. J. 1969 Urethral elasticity and micturition hydrodynamics in females. *Medical and Biological Engineering* **7,** 201–215.

Grotberg, J. B. & Reiss, E. L. 1984 Subsonic flapping flutter. *Journal of Sound and Vibration* **92,** 349–361.

Guyton, A. C. & Adkins, L. H. 1954 Quantitative aspects of the collapse factor in relation to venous return. *American Journal of Physiology* **177,** 523–527.

Hyatt, R. E., Schilder, D. P. & Fry, D. L. 1958 Relationship between maximum expiratory flow and degree of lung inflation. *Journal of Applied Physiology* **13,** 331–336.

Kececioglu, I., McClurken, M. E., Kamm, R. D. & Shapiro, A. H. 1981 Steady, supercritical flow in collapsible tubes. Part 1. Experimental observations. *Journal of Fluid Mechanics* **109,** 367–389.

McClurken, M. E. 1978 Shape-independent area measurement in collapsible tubes by an electrical impedance technique. *Proceedings of the 31st Annual Conference on Engineering in Medicine and Biology*, Atlanta, Georgia, USA, p. 95.

Kamm, R. D., Patel, N. & Elad, D. 1993 On the effect of flow-induced flutter on flow rate during a forced vital capacity maneuver. *FASEB Journal* **7**(3), A11.

Shapiro, A. H. 1977a Steady flow in collapsible tubes. *ASME Journal of Biomechanical Engineering* **99,** 126–147.

Shapiro, A. H. 1977b Physiologic and medical aspects of flow in collapsible tubes. *Proceedings of the 6th Canadian Congress on Applied Mechanics*, Vancouver, B.C., Canada, pp. 883–906.

She, J. 1996 Nonlinear dynamics of forced collapsible tube flow. Ph.D. thesis, University of New South Wales, Sydney, Australia.

Walsh, C., Sullivan, P. A. & Hansen, J. S. 1991 Subcritical flutter in collapsible tube flow: a model of expiratory flow in the trachea. *ASME Journal of Biomechanical Engineering* **113,** 21–26.

Yamane, T. & Orita, T. 1992 Self-excited oscillations with and without supercritical flow in collapsible tubes. *Proceedings of the 7th International Conference on Biomedical Engineering*, 2–4 Dec., Singapore, pp. 502–504.

Yamane, T. & Orita, T. 1994a Relationship of pressure wave velocity to self-excited oscillation of collapsible tube flow. *JSME International Journal Series A* **37,** 71–78.

Yamane, T. & Orita, T. 1994b Hysteresis and multiplicity of collapsible tube flow. *Transactions of the Japan Society of Mechanical Engineers* B **60**-571, 807–812 (in Japanese).

Young, T. 1808 Hydraulic investigations, subservient to an intended Croonian lecture on the motion of the blood. *Philosophical Transactions of the Royal Society* **98,** 164–186.